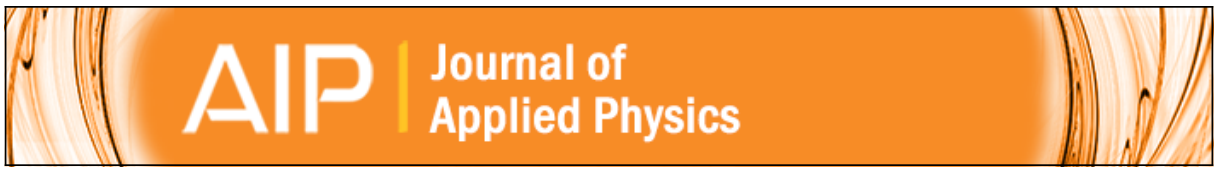

Single ferromagnetic layer magnetic random access memory

M.-J. Xing, M. B. A. Jalil, Seng Ghee Tan, and Y. Jiang

Citation: Journal of Applied Physics **114**, 084306 (2013); doi: 10.1063/1.4819215
View online: http://dx.doi.org/10.1063/1.4819215
View Table of Contents: http://scitation.aip.org/content/aip/journal/jap/114/8?ver=pdfcov
Published by the AIP Publishing

[This article is copyrighted as indicated in the article. Reuse of AIP content is subject to the terms at: http://scitation.aip.org/termsconditions. Downloaded to] IP: 202.6.242.69 On: Fri, 06 Dec 2013 06:23:51

Single ferromagnetic layer magnetic random access memory

M.-J. Xing,[1,2] M. B. A. Jalil,[1,3,a)] Seng Ghee Tan,[1,4] and Y. Jiang[2]
[1]*Computational Nanoelectronics and Nano-device Laboratory, Electronic and Computer Engineering Department, National University of Singapore, Singapore 117576*
[2]*State Key Laboratory for Advanced Metals and Materials, School of Materials Science and Engineering, University of Science and Technology, Beijing 100083, China*
[3]*Information Storage Materials Laboratory, Electronic and Computer Engineering Department, National University of Singapore, Singapore 117576*
[4]*Data Storage Institute, Agency for Science, Technology and Research (A*STAR). DSI Building, 5 Engineering Drive 1, Singapore 117608*

(Received 7 June 2013; accepted 8 August 2013; published online 27 August 2013)

We propose a magnetic random access memory (MRAM) device in which both the writing and reading processes are realized within a single ferromagnetic (FM) layer. The FM layer is sandwiched between layers of heavy element and oxide to enhance the Rashba spin-orbit coupling (RSOC). When the in-plane FM moments are oriented at some intermediate angle to the current direction, the RSOC effect induces a spin accumulation in the FM layer, which in turn generates a Rashba spin torque field via the *s-d* exchange interaction. This field acts as the writing field of the memory device. The RSOC also induces a charge accumulation in the transverse direction via the inverse spin Hall effect (ISHE), which can be used to realize the memory read-out. The writing and read-out processes of the proposed memory are modeled numerically via the non-equilibrium Green's function technique. Besides the advantages of Rashba spin torque writing, i.e., no spin injection and symmetrical data-writing process, this single FM layer MRAM design does away with having a giant magnetoresistive or magnetic tunnel junction multilayer structure by utilizing the ISHE for the read-out process. © *2013 AIP Publishing LLC*. [http://dx.doi.org/10.1063/1.4819215]

I. INTRODUCTION

It has been shown that Rashba spin-orbit coupling (RSOC) effects at the surfaces of metals can be enhanced by the presence of heavy elements[1,2] and surface oxidation.[3] The combination of the enhanced RSOC at the surface, and exchange interactions with the local ferromagnetic (FM) moments result in a large intrinsic spin torque, which is sustained up to room temperature.[4–8] Memory devices which utilize the spin torque effect arising from RSOC has the advantages of higher density of integration and lower energy consumption, as they do not require injection of spin polarized current via non-collinear ferromagnetic layers. In previous works, the read-out process of the proposed RSOC torque based memory is based on the conventional tunnel magnetoresistance effect, which necessitates the presence of a magnetic tunnel junction, thus adding to the device complexity. In this work, we propose the read-out to be based on another phenomenon arising from the RSOC effect, namely the inverse spin Hall effect (ISHE).[9,10] The application of the ISHE in the read-out process enables us to achieve a single layer memory device in which both the writing and reading processes are integrated within the same RSOC medium. The spin Hall effect and its inverse counterpart, ISHE, have been intensively studied in semiconductors.[11–17] However, the integration of Rashba spin torque for writing and intrinsic ISHE for writing in a magnetic random access memory (MRAM) application has not been proposed. Here, we will model numerically via the non-equilibrium Green's function (NEGF) technique both the Rashba torque induced writing process and the read-out process via the Hall voltage induced by the ISHE effect.

Our proposed single FM layer MRAM design is shown schematically in Fig. 1. The key element is the presence of a FM layer with a strong RSOC effect and an in-plane magnetic anisotropy. In general, for a 3*d* FM material, a strong RSOC effect is observed in very thin samples, which exhibit perpendicular anisotropy.[8] However, a recent study of the RSOC effect in 3*d* FM metal system has shown that a significant Rashba field is still present when the FM layer is sufficiently thick to exhibit an in-plane anisotropy.[18] In addition, for 4*f* FM materials like Gd, a large Rashba coupling can coexist with an in-plane anisotropy.[19] In the system under consideration (Fig. 1), the FM layer (Co) is sandwiched between a metal layer made of a heavy element (e.g., platinum) and an oxide layer in order to enhance the RSOC effect at the interfaces. The stable orientation of the FM moments in the Co layer is set along some direction in the *x*-*y* plane, at some angle φ to the current direction along the *x*-axis. The presence of the Rashba SOC induces an effective field H_{eff} along the $\pm y$ direction, depending on the $\pm x$ direction of the current j_x flowing through the FM layer. Thus, by utilizing the Rashba spin torque, the FM moments can be switched symmetrically during the writing process by modulating the direction of the bias voltage and hence that of j_x. Meanwhile, due to the existence of the *x* component of the FM moments, the read-out process can be achieved by measuring the Hall voltage induced by ISHE. We have shown previously[20] that FM moments along the current (i.e., *x*) direction will induce a charge imbalance across half of the length of the top and

a)Author to whom correspondence should be addressed. Electronic mail: elembaj@nus.edu.sg.

 © 2013 AIP Publishing LLC

[This article is copyrighted as indicated in the article. Reuse of AIP content is subject to the terms at: http://scitation.aip.org/termsconditions. Downloaded to] IP: 202.6.242.69 On: Fri, 06 Dec 2013 06:23:51

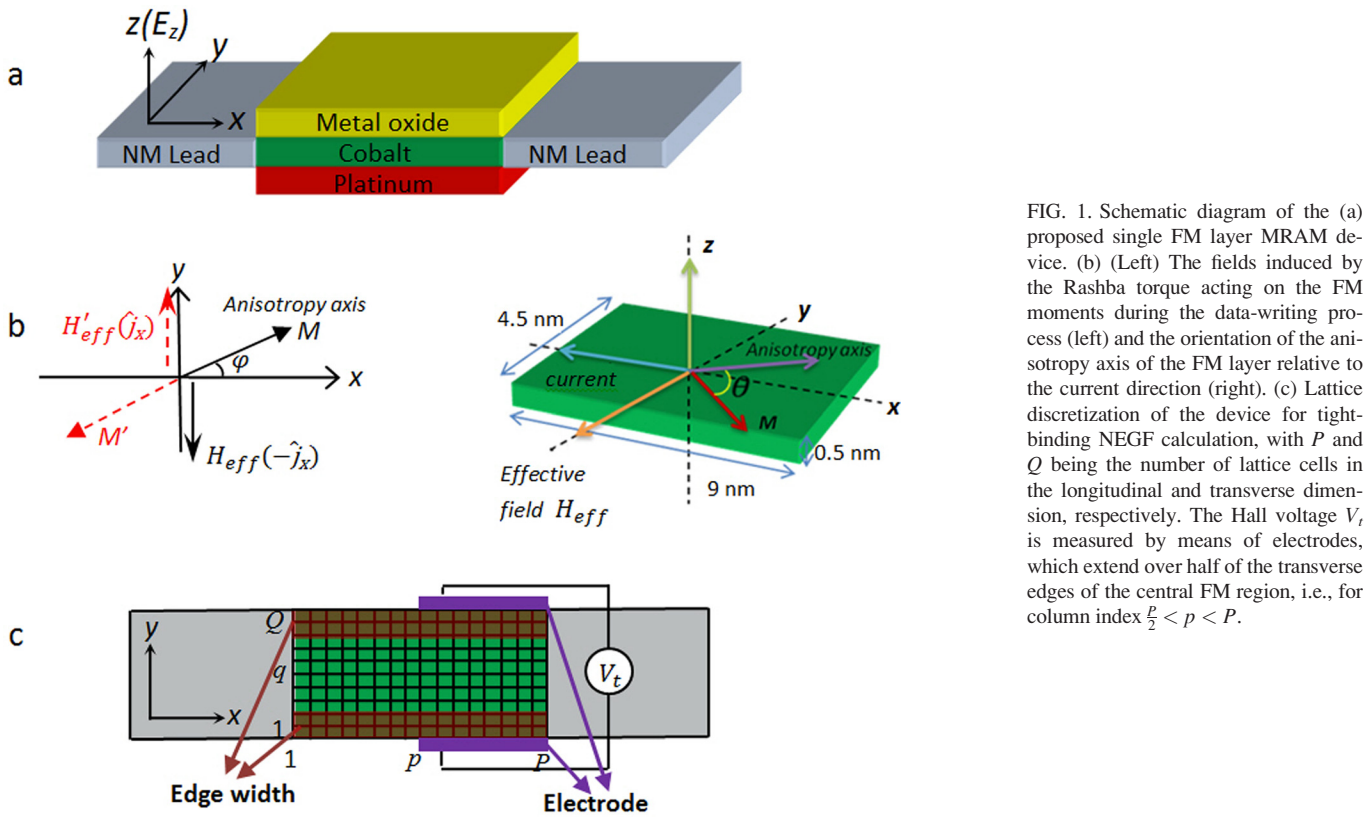

FIG. 1. Schematic diagram of the (a) proposed single FM layer MRAM device. (b) (Left) The fields induced by the Rashba torque acting on the FM moments during the data-writing process (left) and the orientation of the anisotropy axis of the FM layer relative to the current direction (right). (c) Lattice discretization of the device for tight-binding NEGF calculation, with P and Q being the number of lattice cells in the longitudinal and transverse dimension, respectively. The Hall voltage V_t is measured by means of electrodes, which extend over half of the transverse edges of the central FM region, i.e., for column index $\frac{P}{2} < p < P$.

bottom edges, which can be quantified by placing electrodes over the said edges, as shown in Fig. 1(c). Thus, in the device set-up, equilibrium FM orientation (i.e., the easy or anisotropy axis of the FM layer) is set at some intermediate angle $\varphi < \frac{\pi}{2}$ to the current j_x. This will ensure that (i) the magnetization can be switched by the Rashba field, and (ii) the magnetization will induce a charge imbalance along the transverse edge via the ISHE effect.

II. DERIVATION AND CALCULATION

We model the transport of the system via the tight-binding NEGF method.[21] The system is first discretized into a lattice of cells with index (p, q), where $1 \le p \le P$ and $1 \le q \le Q$ [see Fig. 1(c)]. In the tight-binding formalism, the Hamiltonian of the system can be expressed as

$$\begin{aligned}
H_\mu &= \sum_{pq\sigma} 4t_0 a^\dagger_{pq\sigma} a_{pq\sigma} - t_0 (a^\dagger_{p+1,q\sigma} a_{pq\sigma} + a^\dagger_{p,q+1\sigma} a_{pq\sigma} + H.C.) \\
H_C &= \sum_{pq\sigma} \{4t_0 d^\dagger_{pq\sigma} d_{pq\sigma} + J_{sd}[iSgn[\sigma]\sin(\varphi) + \cos(\varphi)] d^\dagger_{pq\bar{\sigma}} d_{pq\sigma} \\
&\quad - t_0 (d^\dagger_{p+1,q\sigma} d_{pq\sigma} + d^\dagger_{p,q+1\sigma} d_{pq\sigma} + H.C.)\} \\
&\quad - it_{so} \sum_{pq\sigma\sigma'} \{[d^\dagger_{p+1,q\sigma} (\hat{\sigma}_y)_{\sigma\sigma'} d_{pq\sigma'} \\
&\quad - d^\dagger_{p,q+1\sigma} (\hat{\sigma}_x)_{\sigma\sigma'} d_{pq\sigma'} + H.C.]\}, \\
H_T &= \sum_{q\sigma} [t'_L a^\dagger_{q\sigma,L} d_{q\sigma,C} + t'_R a^\dagger_{q\sigma,R} d_{q\sigma,C} + H.C.], \qquad (1)
\end{aligned}$$

where H_μ is the Hamiltonian for the non-magnetic (NM) leads ($\mu = L, R$), H_C is the Hamiltonian of the central FM region in the presence of a RSOC effect, which is characterized by the parameter t_{so}, and an exchange interaction between the conduction electrons with the local FM moments, which is characterized by J_{sd} (i.e., $H_M = J_{sd}\,\hat{\boldsymbol{\sigma}} \cdot \hat{\boldsymbol{M}}$ is the exchange Hamiltonian), and H_T is the tunnel coupling between the leads and the central region.

With the above Hamiltonian, one can write the Green's function equation in matrix form: $(E[I] - [H])[G]^r = I$. From this matrix relation, one obtains a series of equations by considering different lattice points (p, q) in the central region, i.e.,

$$\begin{aligned}
I &= (E - 4t_0) G^{q,q}_{p,p}(\sigma\sigma) - J_{sd}[iSgn[\sigma]\sin(\varphi) + \cos(\varphi)] G^{q,q}_{p,p}(\bar{\sigma}\sigma) \\
&\quad + t_0 [G^{q,q}_{p-1,p}(\sigma\sigma) + G^{q,q}_{p+1,p}(\sigma\sigma) + G^{q-1,q}_{p,p}(\sigma\sigma) + G^{q+1,q}_{p,p}(\sigma\sigma)] \\
&\quad - t_{so} [\sigma G^{q,q}_{p+1,p}(\bar{\sigma}\sigma) + iG^{q+1,q}_{p,p}(\bar{\sigma}\sigma) - \sigma G^{q,q}_{p-1,p}(\bar{\sigma}\sigma) \\
&\quad - iG^{q-1,q}_{p,p}(\bar{\sigma}\sigma)]. \qquad (2)
\end{aligned}$$

The infinitely large matrix $[H]$ consists of sub-matrices denoting the Hamiltonian of the central region ($[H_C]$), and that of the two leads, as well as the coupling coefficients between the two leads and the central region ($[\tau_{L/R,C}]$). Following standard tight-binding method procedures, one can represent the effect of the leads in terms of self-energies $[\Sigma]^r_{L,R}$ and obtain a relation for the retarded Green's function of the central region $[G_C]^r$

$$(E[I] - [H_C] - [\Sigma]^r_L - [\Sigma]^r_R)[G_C]^r = I, \qquad (3)$$

where $[\Sigma^{q,q'}_{p,p}]^r_{L(R)} = [\tau]^{q,q}_{p,0(p+1)} [g^r]^{q,q'}_{0(p+1),0(P+1)} [\tau]^{q',q'}_{0(p+1),p}$ are the self energies of the left (L) and right (R) leads, and $[g^r]^{q,q'}_{0(p+1),0(p+1)}$ are the retarded Green's functions of the

[This article is copyrighted as indicated in the article. Reuse of AIP content is subject to the terms at: http://scitation.aip.org/termsconditions. Downloaded to] IP: 202.6.242.69 On: Fri, 06 Dec 2013 06:23:51

isolated L and R leads. The retarded Green's function of the central region can then be evaluated by inverting Eq. (3), i.e., $[G_C]^r = (E[I] - [H_C] - [\Sigma]_L^r - [\Sigma]_R^r)^{-1}$. The lesser Green's function $[G]^<$, which is related to the electron density, can then be calculated via the Langreth formula: $[G]^< = [G]^r[\Sigma]^<[G]^a$ in which $[\Sigma]^< = \sum_{\mu=L,R}([\Sigma]_\mu^a - [\Sigma]_\mu^r)f_\mu$, where f_μ being the Fermi distribution function within lead μ. From the retarded and lesser Green's functions of the central region, one can calculate useful parameters, which are related to the writing and reading processes of the proposed single FM layer MRAM device.

In our numerical calculations, the central region is discretized into a square lattice of $(P \times Q)$ of unit cells, with the cell dimension being set to $a = 0.045$ nm. Since the Fermi energy of the central Co layer is 7.38 eV, the Fermi wavelength $\lambda \approx 10a$, and thus our model can simulate a continuum system to a good approximation. In our calculations, we consider a central region consisting of (200×100) cells, which correspond to the dimensions of $(9\,\text{nm} \times 4.5\,\text{nm})$ for the central region. The other parameters assumed in our calculations are as follows: the coupling strength between neighboring sites is $t = \frac{\hbar^2}{2m^*a^2} = 18.69$ eV, the coupling to the leads are set for simplicity to $t_{L/R} = 0.8t$, and the FM exchange energy is assumed to be $|M| = 0.85$ eV.[22] Now, the typical strength of the RSOC constant α is found to be in the range of $4 \times 10^{-11} < \alpha < 3 \times 10^{-10}$ eVm.[2,19,23] This translates to a range of the RSOC coupling term, $t_{so} = \frac{\alpha}{2a}$ of 0.4 to 3.3 eV. Finally, we assume the easy axis in the central region to lie at the angles $\varphi = \frac{\pi}{6}$ and $\frac{7\pi}{6}$ to the x-axis. These two directions correspond to the magnetization states, which are approximately parallel and antiparallel to the x-direction, respectively, but with a component along the y-axis to enable switching via the Rashba spin torque.

A. Writing process based on Rashba spin torque switching

The effect of Rashba spin torque on magnetization dynamics has been theoretically studied[4–7] and experimentally confirmed.[8] However, these previous results cannot be utilized directly for MRAM application, because the effective field (H_{eff}) due to RSOC (in the in-plane direction) was directed perpendicular to the equilibrium orientation of the FM moments (in the out-of-plane direction). Thus, the field H_{eff} due to the RSOC effect did not break the symmetry between the two stable orientations of the FM magnetization and could not switch it from one stable direction to the other. To overcome this limitation in our proposed device, where the easy direction is set at an in-plane direction, at some angle $\varphi < \frac{\pi}{2}$ to the H_{eff} direction (along the y-axis)—see Fig. 1(b).

We now set out to calculate the effective field acting on the FM moments in the central region due to the Rashba spin torque. From the NEGF method, we first evaluate the spin accumulation $\langle s_i \rangle$, which is induced by the combined effect of exchange coupling with the local FM moments and the RSOC effect. Then, by considering the exchange energy term in the Hamiltonian, i.e., $H_M = J_{sd}(\hat{S} \cdot M)$, one can deduce H_{eff} by taking the functional derivative (for simplicity we reset $H_{eff} = \mu_0 H_{eff}$)

$$H_{eff}(i) = -\frac{\partial H_M}{\partial M} = -\frac{J_{sd}\langle s_i \rangle}{M_s} = -\frac{J_{sd}\langle s_y \rangle_m}{M_s V} \tag{4}$$

in which $i = x, y, z$ denotes the axis directions, M_s is the saturation magnetization of Co, and V is the volume. Having obtained H_{eff}, the effect of the Rashba torque on the FM magnetization dynamics can be modeled by treating H_{eff} as an additional field. For instance, the switching (writing) of the FM moments can be obtained by minimizing their free energy. The local spin density in Eq. (4) can be evaluated by considering the Green's functions derived in Sec. I. In the cell at (p, q), it is given by

$$\langle s_i \rangle_{pq} = -\frac{i\hbar}{4\pi}\int_{-\infty}^{\infty} Tr[\hat{S}_i G^<_{pq,pq}(E)]dE. \tag{5}$$

The effective field H_{eff} is then estimated by taking the discrete sum over the lattice cells, i.e.,

$$H_{eff}(i) = -\frac{J_{sd}\sum_{pq}\langle s_i \rangle_{pq}}{M_s(PQa^2t)}, \tag{6}$$

where t is the thickness of the Co layer. Besides the effective field, we also calculate the current through the device. From the Hamiltonian, we find that current passing through the device in the $\pm x$ directions will give rise to a Rashba effective field H_{eff} in the $\pm y$ directions (noting that the interfacial electrical field E_z which generates the RSOC effect lies in the z direction as shown in Fig. 1(b)). The charge current through the system can be expressed in terms of the Green's functions as follows:

$$I_\alpha = \frac{e}{h}\int_{-\infty}^{\infty} Tr[[\Sigma]_\alpha^<(\epsilon)A(\epsilon)] - [\Gamma(\epsilon)_\alpha G^<(\epsilon)]d\epsilon, \tag{7}$$

where $A(\epsilon) = i[G^r(\epsilon) - G^a(\epsilon)]$ is the spectral function.

We investigate the correlation between the effective field H_{eff} to the charge current. Fig. 2(a) shows that the effective field H_{eff} in the y-direction is linearly proportional to the current density. Since H_{eff} is primarily induced by the RSOC effect, we expect it to increase with the RSOC strength t_{so}. As shown in Fig. 2(b), H_{eff} does show a generally increasing trend with t_{so} and for a sufficiently large Rashba coupling, the increase is approximately proportional with t_{so}. These trends are consistent with previous results.[4–8]

Having evaluated H_{eff}, we now consider its role in the switching of the FM moments, which constitutes the writing process in our MRAM device. Assuming M is initially along the easy axis, i.e., in one of the two stable states of the FM magnetization, as shown in Fig. 1(b). Upon application of current in the $-x$ direction, M can be made to align to H_{eff} in the y-direction if the current density $-j_x$ is sufficiently large. When the current is switched off, M will then relax to the nearest stable state M'. M' can be switched back to the original stable direction M by applying the bias voltage and hence, current in the opposite direction due to the symmetry of the RSOC effect (i.e., current in the x direction will produce H_{eff} in the $-y$ direction). We model this writing

[This article is copyrighted as indicated in the article. Reuse of AIP content is subject to the terms at: http://scitation.aip.org/termsconditions. Downloaded to] IP: 202.6.242.69 On: Fri, 06 Dec 2013 06:23:51

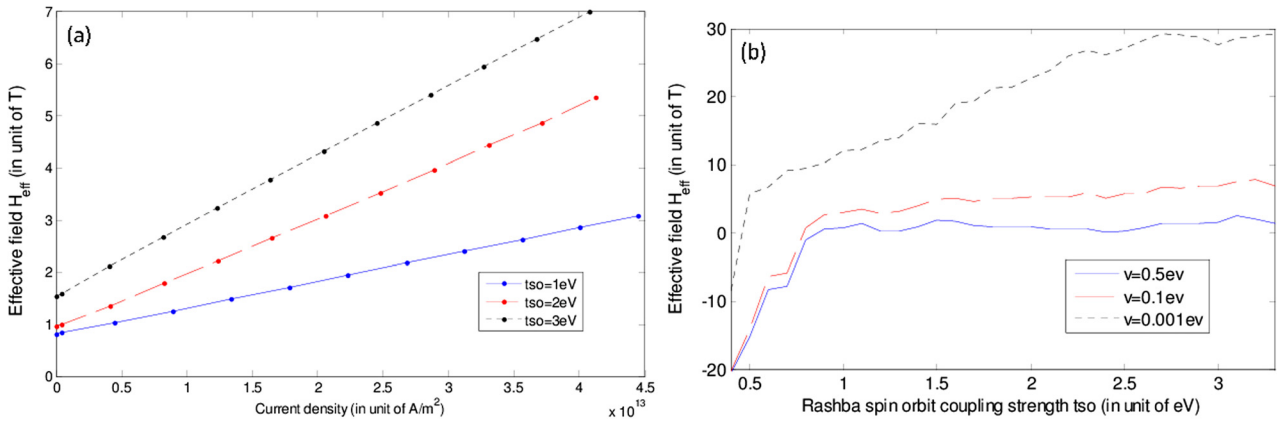

FIG. 2. The effective field H_{eff} in the y-direction as a function of (a) current density in the x-direction for different RSOC strengths, which are characterized by the coupling term t_{so}; and (b) RSOC strength t_{so} for different bias voltage values.

(switching) process by considering the classical free energy expression. By considering the system shown in Fig. 1(b), and assuming it is uniformly magnetized (macrospin model), the free energy is given by

$$\mathcal{E} = K_u \sin^2\theta + M_s H_{eff} \sin(\varphi - \theta) + \frac{1}{2}\mu_0 M_s^2 \sum_{i=x,y,z} N_i m_i^2, \quad (8)$$

where K_u is the anisotropy energy, θ is the angle between the magnetization $\mathbf{M}$ and the easy axis, N_i is the demagnetizing factor along axis i, and m_i are the corresponding direction cosines of $\mathbf{M}$. Let the current, effective field, and the vertical axis to be along the $-x$, $-y$, and z axes, respectively, as shown in Fig. 1(b). If we assume, the magnetization switching to occur within the x-y plane, then the above expression reduces to

$$\mathcal{E} = K_u \sin^2\theta + M_s H_{eff} \sin(\varphi - \theta) + \frac{1}{2}\mu_0 M_s^2 (N_x - N_y)\cos^2(\varphi - \theta) + C, \quad (9)$$

where C is some constant independent of θ. In the above, we assume the demagnetizing factors to be constant. Generally, these factors are constant only for magnets of ellipsoidal shape.[24] For the rectangular FM layer in our structure, the demagnetizing factors would vary spatially. Thus, we estimate the corresponding demagnetizing factors by averaging over the volume of the FM layer. Such an approximation would suffice for the macrospin model adopted in our calculation. The dimensions assumed for the Co layer are ($9\,\text{nm} \times 4.5\,\text{nm} \times 0.5\,\text{nm}$), for which the average demagnetizing factors are numerically given by:[25] $N_z = 0.8278$; $N_x = 0.0563$; and $N_y = 0.1159$. Taking the values for the magnetic parameters of Co as $M_s = 1.09 \times 10^6\,\text{Am}^{-1}$ and $K_u = 1.0028 \times 10^6\,\text{Jm}^{-3}$,[8] we evaluate the equilibrium magnetization direction θ, which corresponds to the minimum energy. Repeating this for different applied field H_{eff} values as H_{eff} is swept from negative to positive saturation and *vice versa*, we obtain the magnetic hysteresis curves corresponding to different easy axis orientation (Fig. 3). The maximum switching field occurs when the anisotropy axis coincides with the long axis of the Co layer (along the x-axis) and is approximately 0.8 T. Referring to Fig. 2(a), one can see that this switching field can be attained at a current density of less than 1.0×10^9 A/cm^2 for the range of Rashba coupling strengths considered.

B. Reading process based on ISHE

The non-equilibrium charge density $\rho_{p,q}$ in the central region is given by

$$\rho_{p,q} = -\frac{ie}{2\pi t a^2}\int_{-\infty}^{\infty} Tr[G^{<}_{pq,pq}(E)]dE, \quad (10)$$

where (p, q) corresponds to the lattice coordinates in Fig. 1(b), t is the thickness of the central region, a is the lattice constant, and the trace is performed over the spin degree of freedom. The Hall voltage is reflected, up to a proportionality constant, by the charge density difference at the top and bottom boundaries of the right half of the central region over which the Hall electrode extends, i.e., for column index $\frac{P}{2} < p < P$ [see Fig. 1(c)]. In the case of the spin Hall effect, there is an imbalance only in the spins but not charge, and thus the charge density difference $\Delta\rho = 0$. In our case, however, the presence of the net x-component FM moment results in a nonzero $\Delta\rho$ due to ISHE.[20] The sign of $\Delta\rho$, and hence the Hall voltage V_t is dependent on the magnetization

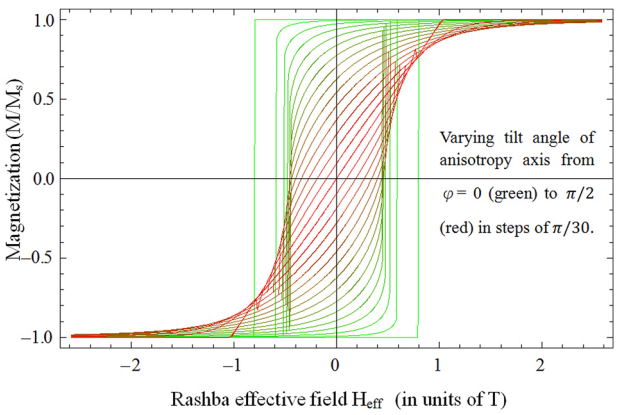

FIG. 3. Magnetic hysteresis of the FM layer for different tilt angles φ of the anisotropy axis.

[This article is copyrighted as indicated in the article. Reuse of AIP content is subject to the terms at: http://scitation.aip.org/termsconditions. Downloaded to] IP: 202.6.242.69 On: Fri, 06 Dec 2013 06:23:51

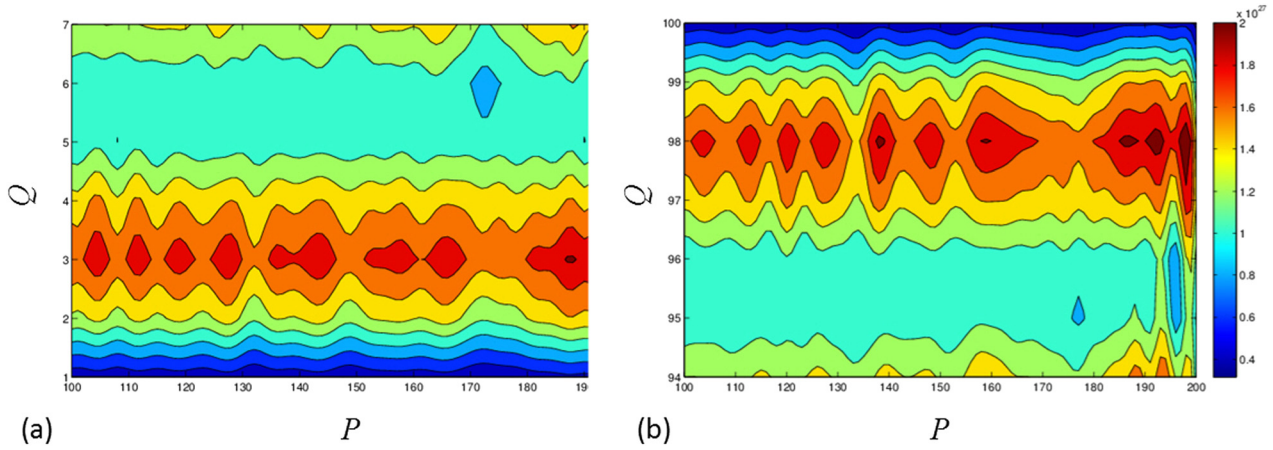

FIG. 4. The charge distribution $\rho_{p,q}$ (in unit of $\frac{e}{m^3}$) at the (a) bottom, and (b) top edges of the right-hand half of a central region discretized into a lattice of $(P \times Q) = (200 \times 100)$ cells, corresponding to the magnetization orientation of $\varphi = \frac{\pi}{6}$ to the x-axis. The RSOC strength is $t_{so} = 0.9$ eV and the bias voltage is $V = 1$ meV.

orientation φ with respect to the x-axis. Hence, when the FM moments are switched from $\frac{\pi}{6}$ to $\frac{7\pi}{6}$, this will be accompanied by the reversal in the sign of V_t. Fig. 4 shows the calculated charge distribution of $\rho_{p,q}$ at (a) the bottom, and (b) top edges of the right half of the central region, corresponding to the RSOC strength of $t_{so} = 0.9$ eV and a small bias voltage of $V = 1$ meV. The bias voltage is chosen such that the charge current is not sufficiently large to switch the FM moments, according to the results in Subsection II A. Even at this small bias voltage, there is a distinct charge accumulation at the top edge when the magnetization is oriented at $\varphi = \frac{\pi}{6}$ as can be seen in the asymmetry between Figs. 4(a) and 4(b). When the magnetization is switched from $\frac{\pi}{6}$ to $\frac{7\pi}{6}$, the charge imbalance shifts to the bottom edge, and thus the sign of V_t reverses.

Finally, we would like to estimate the size of the Hall voltage. Applying Coulomb's law, the Hall voltage would be proportional to the linear density of the charge imbalance at the edges, and inversely proportional to the transverse width of the Co layer. Using this fact and a previous Hall voltage study of Rashba SOC in semiconductors,[16] and noting the electron density of the order of $10^{26}\, e/\mathrm{m}^3$ [see Figs. 4(a) and 4(b)] and the dimensions of the Co layer (Fig. 1), we estimate a sizable Hall voltage of the order of 1.0 V, which should be readily measurable. Hence, this shows that the ISHE can generate a readable Hall voltage, which is dependent on the orientation of the magnetization, and thus be utilized in the readback process of our proposed single layer memory device.

III. CONCLUSION

In summary, we have proposed a single FM layer MRAM device, which utilizes the Rashba spin torque effect to switch the FM magnetization for the writing process, and the voltage generated by the ISHE for the read-out process. The critical parameters for the writing and reading processes, i.e., the effective field due to the Rashba torque and the charge accumulation at the transverse edges due to ISHE, respectively, were determined numerically via the non-equilibrium Green's function technique. These calculations coupled with the macrospin calculation of the switching field of the FM element indicate the feasibility of utilizing the Rashba torque and ISHE effects to integrate the writing and reading processes within a single FM layer. The single FM layer MRAM design combines the advantages of Rashba spin torque writing, i.e., no requirement of spin injection and symmetrical data-writing process, with a simpler device design, as the giant magnetoresistive (GMR) stack or magnetic tunnel junction structure is not required for the read-out process.

ACKNOWLEDGMENTS

This work was supported by the ASTAR SERC Grant No. 092 101 0060 (R-398-000-061-305) and the NSFC Grant Nos. 50831002 and 51071022.

[1]P. Gambardella, S. Rusponi *et al.*, Science **300**, 1130 (2003).
[2]C. R. Ast, J. Henk *et al.*, Phys. Rev. Lett. **98**, 186807 (2007).
[3]S. LaShell, B. A. McDougall, and E. Jensen, Phys. Rev. Lett. **77**, 3419 (1996).
[4]S. G. Tan, M. B. A. Jalil, and X. J. Liu, e-print arXiv:0705.3502 (2007).
[5]S. G. Tan, M. B. A. Jalil, T. Fujita, and X. J. Liu, Ann. Phys. **326**, 207, (2011).
[6]A. Manchon and S. Zhang, Phys. Rev. B **78**, 212405 (2008).
[7]K. Obata and G. Tatara, Phys. Rev. B **77**, 214429 (2008).
[8]I. M. Miron, G. Gaudin, S. Auffret, B. Rodmacq, A. Schuhl, S. Pizzini, J. Vogel, and P. Gambardella, Nature Mater. **9**, 230 (2010).
[9]S. Murakami, N. Nagaosa, and S.-C. Zhang, Science **301**, 1348 (2003).
[10]J. Sinova *et al.*, Phys. Rev. Lett. **92**, 126603 (2004).
[11]S. O. Valenzuela and M. Tinkham, Nature **442**, 176 (2006).
[12]E. Saitoh, M. Ueda, H. Miyajima, G. Takahashi, and S. Maekawa, Appl. Phys. Lett. **88**, 182509 (2006).
[13]T. Kimura, Y. Otani, T. Sato, S. Takahashi, and S. Maekawa, Phys. Rev. Lett. **98**, 156601 (2007).
[14]E. M. Hankiewicz, J. Li, T. Jungwirth, Q. Niu, S. Q. Shen, and J. Sinova, Phys. Rev. B **72**, 155305 (2005).
[15]Y. Xing, Q.-F. Sun, and J. Wang, Phys. Rev. B **75**, 075324 (2007).
[16]J. Li and S.-Q. Shen, Phys. Rev. B **76**, 153302 (2007).
[17]J. J. Zhang, F. Liang, and J. Wang, Eur. Phys. J. B **72**, 105 (2009).
[18]X. Fan, J. Wu, Y. Chen, M. J. Jerry, H. Zhang, and J. Q. Xiao, Nat. Commun. **4**, 1799 (2013).
[19]O. Krupin *et al.*, Phys. Rev. B **71**, 201403(R) (2005).
[20]M.-J. Xing, M. B. A. Jalil, S. G. Tan, and Y. Jiang, AIP Adv. **2**, 032147 (2012).
[21]S. Datta, *Electronic Transport in Mesoscopic Systems* (Cambridge, 1995).
[22]S. Wakoh and J. Yamashita, J. Phys. Soc. Jpn. **28**, 1151 (1970).
[23]J. Henk *et al.*, J. Phys.: Condens. Matter **16**, 7581 (2004).
[24]A. Aharoni, *Introduction to the Theory of Ferromagnetism* (Oxford University Press, 2001).
[25]A. Aharoni, J. Appl. Phys. **83**, 3432 (1998).

[This article is copyrighted as indicated in the article. Reuse of AIP content is subject to the terms at: http://scitation.aip.org/termsconditions. Downloaded to] IP: 202.6.242.69 On: Fri, 06 Dec 2013 06:23:51